Eur. Phys. J. C (2022) 82:474
https://doi.org/10.1140/epjc/s10052-022-10402-0

THE EUROPEAN PHYSICAL JOURNAL C

Regular Article - Theoretical Physics

Interdependence of the new "MUON G-2" result and the W-boson mass

Emanuele Bagnaschi[1,a], **Manimala Chakraborti**[2,b], **Sven Heinemeyer**[3,c], **Ipsita Saha**[4,d], **Georg Weiglein**[5,6,e]

[1] CERN, Theoretical Physics Department, 1211 Geneva 23, Switzerland
[2] Astrocent, Nicolaus Copernicus Astronomical Center of the Polish Academy of Sciences, ul. Rektorska 4, 00-614 Warsaw, Poland
[3] Instituto de Física Teórica (UAM/CSIC), Universidad Autónoma de Madrid, 28049 Cantoblanco, Madrid, Spain
[4] Kavli IPMU (WPI), UTIAS, University of Tokyo, Kashiwa, Chiba 277-8583, Japan
[5] Deutsches Elektronen-Synchrotron DESY, Notkestr. 85, 22607 Hamburg, Germany
[6] Universität Hamburg, Luruper Chaussee 149, 22761 Hamburg, Germany

Received: 26 April 2022 / Accepted: 5 May 2022 / Published online: 23 May 2022

Abstract The electroweak (EW) sector of the Minimal Supersymmetric extension of the Standard Model (MSSM), assuming the lightest neutralino as Dark Matter (DM) candidate, can account for a variety of experimental results. This includes the DM direct detection limits, the searches for EW superpartners at the LHC, and in particular the discrepancy between the experimental result for the anomalous magnetic moment of the muon, $(g-2)_\mu$, and its Standard Model (SM) prediction. The new "MUON G-2" result, combined with the older BNL result on $(g-2)_\mu$, yields a deviation from the SM prediction of $\Delta a_\mu = (25.1 \pm 5.9) \times 10^{-10}$, corresponding to $4.2\,\sigma$. Using this updated bound, together with the other constraints, we calculate the MSSM prediction for the mass of the W boson, M_W. We assume contributions only from the EW sector, i.e. the colored sector of the MSSM, in agreement with the search limits, is taken to be heavy. We investigate five scenarios, distinguished by the mechanisms which yield a relic DM density in agreement with the latest Planck bounds. We find that with the new $(g-2)_\mu$ result taken into account and depending on the scenario, values up to $M_W^{\rm MSSM} \lesssim 80.376$ GeV are reached. The largest values are obtained for wino DM and in the case of slepton co-annihilation, where points well within the $1\,\sigma$ range of the experimental world average of $M_W^{\rm exp} = 80.379 \pm 0.012$ GeV are reached, whereas the SM predicts a too small value of $M_W^{\rm SM} = 80.353$ GeV. We analyze the dependence of $M_W^{\rm MSSM}$ on the relevant masses of the EW superpartners and demonstrate that future M_W measurements, e.g. at the ILC, could distinguish between various MSSM realizations. Sizable contributions to $M_W^{\rm MSSM}$ are associated with a relatively light $\tilde{\chi}_1^0$, accompanied by either a light chargino or a light smuon, setting interesting targets for future collider searches.

1 Introduction

Recently the "MUON G-2" collaboration [1] published the results of their Run 1 data [2] of the anomalous magnetic moment of the muon, $a_\mu := \frac{1}{2}(g-2)_\mu$, which is within $0.8\,\sigma$ in agreement with the older BNL result on $(g-2)_\mu$. The combination of the two results yields

$$a_\mu^{\rm exp} = (11659206.1 \pm 4.1) \times 10^{-10} \,. \tag{1}$$

The Standard Model (SM) prediction of a_μ is given by [3] (based on Refs. [4–23]),

$$a_\mu^{\rm SM} = (11659181.0 \pm 4.3) \times 10^{-10} \,. \tag{2}$$

Accordingly, the discrepancy between the experimental value and the SM prediction amounts to

$$\Delta a_\mu \equiv a_\mu^{\rm exp} - a_\mu^{\rm SM} = (25.1 \pm 5.9) \times 10^{-10} \,, \tag{3}$$

corresponding to a $4.2\,\sigma$ discrepancy. At the time of the announcement of the MUON G-2 result, also a new lattice calculation for the leading order hadronic vacuum polarization (LO HVP) contribution to $a_\mu^{\rm SM}$ [24] has been published. This result, however, had not been used in the new theory world average, Eq. (2) [3]. In our analysis below we use Δa_μ as given in Eq. (3). The comparison of the new lattice

[a] e-mail: Emanuele.Bagnaschi@cern.ch (corresponding author)
[b] e-mail: mani.chakraborti@gmail.com
[c] e-mail: Sven.Heinemeyer@cern.ch
[d] e-mail: ipsita.saha@ipmu.jp
[e] e-mail: Georg.Weiglein@desy.de

result with previous results in the literature and the assessment of the uncertainty estimate used in Ref. [24] are still a matter of debate, see e.g. Refs. [25,26]. Possible implications of the new lattice result for the way physics beyond the SM (BSM) could manifest itself were discussed in Refs. [27,28]. The impact of the new result for $a_\mu^{\rm exp}$ on possible scenarios of BSM physics that address its deviation from the SM prediction will clearly depend on how the theoretical prediction within the SM will settle during the next years. If a discrepancy at the level of Eq. (3) (or even stronger) will be confirmed by future theoretical and experimental analyses, a_μ will be a key observable for narrowing down the possible nature of BSM physics.

Among the BSM theories under consideration for accommodating a deviation at the level of Eq. (3), the Minimal Supersymmetric extension of the Standard Model (MSSM) [29–32] is one of the most prominent candidates. Supersymmetry (SUSY) predicts the existence of two scalar partners for each SM fermion as well as fermionic partners for all SM bosons. Contrary to the case of the SM, the theoretical structure of the MSSM requires two Higgs doublets. This results in five physical Higgs bosons instead of the single Higgs boson in the SM. In the $\mathcal{CP}$-conserving case, considered in this article, these are the light and heavy $\mathcal{CP}$-even Higgs bosons, h and H, the $\mathcal{CP}$-odd Higgs boson, A, and the charged Higgs bosons, $H^\pm$. The neutral SUSY partners of the neutral Higgs and electroweak (EW) gauge bosons give rise to the four neutralinos, $\tilde\chi^0_{1,2,3,4}$. The corresponding charged SUSY partners are the charginos, $\tilde\chi^\pm_{1,2}$. The SUSY partners of the SM leptons and quarks are the scalar leptons and quarks (sleptons, squarks), respectively.

In Refs. [33–36] some of us performed an analysis of the EW sector of the MSSM, taking into account all relevant experimental data, i.e. data that is directly connected to the EW sector. It was assumed that the Lightest SUSY Particle (LSP) is the lightest neutralino, $\tilde\chi^0_1$, with the requirement that it is in agreement with the bounds on the Dark Matter (DM) content of the universe [37,38]. The experimental results employed in the analyses of Refs. [33–36] comprise the direct searches at the LHC [39,40], the DM relic abundance [41], the DM direct detection experiments [42–44] together with the deviation on the value of the anomalous magnetic moment of the muon. [1]

In Refs. [33–36] five different scenarios were analyzed, classified by the mechanism that has the main impact on the resulting LSP relic density. The scenarios differ by the nature of the Next-to-LSP (NLSP). They comprise $\tilde\chi^\pm_1$-coannhiliation, $\tilde l^\pm$-coannihilation with either "left-" or "right-handed" sleptons close in mass to the LSP ("case-L" and "case-R", respectively), wino DM, as well as higgsino DM. In the first three scenarios the full amount of DM can be provided by the MSSM, whereas in the latter two cases the measured DM density serves as an upper limit. Requiring Eq. (3) at the $2\,\sigma$ level, together with the collider and DM constraints, results in upper limits on the LSP masses at the level of $\sim$ 500 GeV to $\sim$ 600 GeV for all five scenarios. Corresponding upper limits on the mass of the NLSP are obtained for only slightly higher mass values.

It is interesting to note that there is another EW high-precision observable that shows a (slight) discrepancy between the experimental result and the SM prediction, namely the mass of the W boson, M_W. The experimental world average is [45]

$$M_W^{\rm exp} = 80.379 \pm 0.012 \text{ GeV} , \tag{4}$$

whereas the SM predicts a value of

$$M_W^{\rm SM} = 80.353 \pm 0.004 \text{ GeV} . \tag{5}$$

For the central value of $M_W^{\rm SM}$ we use the implementation in the code `FeynHiggs` [46–48] (see below for details), while the quoted theoretical uncertainty is based on an estimate of unknown higher-order corrections [49] (in a comparison of the result in the here used on-shell scheme with a result in the $\overline{\rm MS}$ scheme a difference of 6 MeV was reported [50]). It is expected that this uncertainty can be reduced to $\sim$ 0.001 GeV within the next decades, see Ref. [51,52] and references therein.

Concerning the MSSM, in Refs. [53–55] it was shown that EW SUSY particles alone, provided that they are sufficiently light, can induce significant shifts in the $M_W^{\rm MSSM}$ prediction w.r.t. $M_W^{\rm SM}$ (taking into account the then valid lower limits on the EW SUSY masses). Those results motivate a combined analysis investigating whether the discrepancy in a_μ as given in Eq. (3) and the difference between the current value of $M_W^{\rm exp}$ as given in Eq. (4) and the SM prediction of Eq. (5) could arise from loop corrections of the same type of SUSY particles. While many papers interpreted the observed $(g-2)_\mu$ discrepancy of $4.2\,\sigma$ in SUSY models [33–36,56–118], none of those papers analyzed M_W in this context.

In the present paper we analyze the prediction of $M_W^{\rm MSSM}$ in view of the new world average of $a_\mu^{\rm exp}$. We focus on the five MSSM scenarios presented in Refs. [33,34], well motivated by DM constraints and characterized by relatively light EW SUSY particles and a heavy colored supersymmetric spectrum. Since the squarks and the gluino are assumed to be heavy in those scenarios, in agreement with the experimental bounds from direct searches, they yield a negligible contribution to $M_W^{\rm MSSM}$. All analyzed parameter points are in agreement with the experimental result on the relic DM density, which is imposed as an upper bound (for the scenarios

[1] In Refs. [33,34] the previous experimental result based on Refs. [12,13] was used, while Ref. [33] was updated with the new world average on $(g-2)_\mu$ in Ref. [35].

with $\tilde{\chi}_1^\pm$-coannhiliation and $\tilde{l}^\pm$-coannihilation for case-L and case-R this bound can be saturated, while for the scenarios with wino DM and higgsino DM the obtained relic density stays below the measured value), with DM direct detection bounds, and with LHC searches for light EW SUSY particles. In these scenarios we investigate the prediction for $M_W^{\rm MSSM}$ in combination with the contribution to $\Delta a_\mu^{\rm MSSM}$ w.r.t. the new value for the discrepancy Δa_μ as given in Eq. (3). We assess how well the MSSM prediction agrees with the current experimental value for $M_W^{\rm exp}$. We analyze the dependence on the relevant masses and parameters in the MSSM. Finally we briefly discuss the impact of potential precision measurements of $M_W^{\rm exp}$ at future e^+e^- colliders such as the ILC, FCC-ee or CEPC.

The paper is organized as follows. In Sect. 2 we give a brief description of the sectors of the MSSM relevant for our analysis. We review the experimental constraints applied to the MSSM parameter space and give a description of our calculation of $M_W^{\rm MSSM}$. In the last part of this section we briefly review the five scenarios that are analyzed in this paper. The numerical results for the $M_W^{\rm MSSM}$ prediction in our scenarios, together with an analysis of the relevant parameter dependences is given in Sect. 3. We conclude in Sect. 4.

2 The model, experimental constraints and M_W

2.1 The model

A detailed description of our conventions used for the EW sector of the MSSM can be found in Ref. [33]. Here we just list the input parameters and masses that are relevant for our analysis. Throughout this paper we assume that all parameters are real, i.e. we do not incorporate possible $\mathcal{CP}$-violating effects that can be induced via SUSY loop corrections with complex parameters.

The masses and mixings of the charginos and neutralinos are determined by $U(1)_Y$ and $SU(2)_L$ gaugino soft SUSY-breaking mass parameters M_1 and M_2, the Higgs/higgsino mass parameter μ, and $\tan\beta$, the ratio of the vacuum expectation values (vevs) of the two Higgs doublets of the MSSM, $\tan\beta \equiv v_2/v_1$. The four neutralino masses are ordered as $m_{\tilde{\chi}_1^0} < m_{\tilde{\chi}_2^0} < m_{\tilde{\chi}_3^0} < m_{\tilde{\chi}_4^0}$. Similarly, the two chargino-masses are denoted as $m_{\tilde{\chi}_1^\pm} < m_{\tilde{\chi}_2^\pm}$. As explained in Ref. [33], it is sufficient for our analysis to focus on positive values for M_1, M_2 and μ.

For the sleptons, as in Ref. [33], we choose common soft SUSY-breaking parameters for all three generations, $m_{\tilde{l}_L}$ and $m_{\tilde{l}_R}$. We take the trilinear coupling A_l ($l = e, \mu, \tau$) to be zero. We follow the convention that $\tilde{l}_1$ ($\tilde{l}_2$) has the large "left-handed" ("right-handed") component. Besides the symbols that refer to equal values for all three generations, $m_{\tilde{l}_1}$ and $m_{\tilde{l}_2}$, we also explicitly use the scalar electron, muon and tau masses, $m_{\tilde{e}_{1,2}}$, $m_{\tilde{\mu}_{1,2}}$ and $m_{\tilde{\tau}_{1,2}}$.

We assume that the colored sector of the MSSM is significantly heavier than the EW sector, and does not play a role in this analysis since it yields a negligible contribution to $a_\mu^{\rm MSSM}$ and $M_W^{\rm MSSM}$. Since the colored particles are assumed to be very heavy, they are not affected by the LHC limits from direct searches [39,40]. In particular we have chosen the scalar top/bottom sector parameters in such a way that the radiative corrections to the mass of the light $\mathcal{CP}$-even Higgs boson yield a value in agreement with the experimental data, $M_h \sim 125$ GeV (taking into account a theory uncertainties of ± 3 GeV, which as a conservative estimate amounts to about twice the value obtained in Ref. [119]). The determination of the stop/sbottom MSSM parameters has been performed with `FeynHiggs-2.18.0` [46–48,119–124]. The resulting stop masses are found to be heavier than 2 TeV [125,126], in agreement with the above assumption of a heavy colored sector.

The mass of the $\mathcal{CP}$-odd Higgs boson, M_A, has been assumed to be heavy ($\gtrsim$ 2 TeV) which ensures its compatibility with the experimental bounds from the LHC. As a consequence, effects from H-/A-pole annihilation of DM in the early universe are absent in our analysis.

2.2 Relevant constraints

Concerning the experimental constraints taken into account, we follow Ref. [33]. These comprise

- Vacuum stability constraints:

  All points are checked to possess an EW vacuum that has the correct properties and is stable, e. g. avoiding charge and color breaking minima. This check is performed with the public code `Evade` [127,128].
- Constraints from the LHC and LEP:

  EW SUSY searches at the LHC are taken into account as described in Ref. [33]. This has mostly been done via `CheckMATE` [129–131], where many analyses were newly implemented [33]. In this context also the code `SDECAY` [132] as in included in `SUSYHIT-1.5a` has been used. The points are furthermore required to satisfy the $\tilde{\chi}_1^\pm$ mass limit from LEP [133].
- Dark matter relic density constraints:

  We use the latest result from Planck [41] as an upper limit. The relic density in the MSSM is evaluated with `MicrOMEGAs-5.0.8` [134–137].
- Dark matter direct detection constraints:

  We employ the constraint on the spin-independent DM scattering cross-section $\sigma_p^{\rm SI}$ from the XENON1T [42]

experiment, evaluating the theoretical prediction for $\sigma_p^{\rm SI}$ using `MicrOMEGAs`. A combination with other direct detection experiments would yield only very slightly stronger limits, with a negligible impact on our results.
- We indicate in the plots the new result for Δa_μ as given in Eq. (3), which is applied at the $\pm 2\sigma$ level as a constraint that the parameter points have to pass. The evaluation has been done with the code `GM2Calc-1.7.5` [138], incorporating two-loop corrections from Refs. [139–141] (see also Refs. [142,143]).

In addition, we have verified using `HiggsSignals-2.6.1` [144–146] that the properties of the Higgs state at $\sim$ 125 GeV, which could be modified by presence of light SUSY EW states, are in agreement with the current measurements.

2.3 The W-boson mass

The mass of the W boson can be predicted from muon decay, which relates M_W to three extremely precisely measured quantities, namely the Fermi constant, G_μ, the fine structure constant, α, and the mass of the Z boson, M_Z. Within the SM and many extensions of it, in particular the MSSM, this relation can be used to predict M_W via the expression [2]

$$M_W^2 = M_Z^2 \times \left\{ \frac{1}{2} + \sqrt{\frac{1}{4} - \frac{\pi\,\alpha}{\sqrt{2}\,G_\mu\,M_Z^2}\,[1 + \Delta r(M_W, M_Z, m_t, \ldots)]} \right\}, \tag{6}$$

where the quantity Δr is zero at lowest order. It comprises loop corrections to muon decay in the considered model, where the ellipsis in Eq. (6) denotes the specific particle content of the model. Since Δr is a function of M_W itself, it is convenient to evaluate Eq. (6) via an iterative procedure.

The SM prediction for Δr includes contributions at the complete one-loop [148,149] and the complete two-loop level [150–165], as well as partial higher-order corrections up to four-loop order [166–175]. [3] Our prediction for M_W in the MSSM is based on the full one-loop result for Δr [53–55] (see also Ref. [180]), supplemented by the leading two-loop corrections [181–183]. The leading one- and two-loop contributions arise from isospin splitting between different SUSY particles and enter via the quantity $\Delta\rho$, which receives contributions from the W-boson and Z-boson self-energies at vanishing external momentum. At the one-loop level the squarks enter only via self-energy contributions, i.e. predominantly via $\Delta\rho$. The same is true for the corresponding contribution of pure slepton loops, while the contributions of the chargino and neutralino sector enter also via vertex and box diagrams. In our MSSM prediction for M_W the contributions involving SUSY particles are combined with all available SM-type contributions up to the four-loop level as described above. This ensures that the state-of-the-art SM prediction is recovered in the decoupling limit where all SUSY mass scales are heavy. For our analysis we use the implementation of the SM and SUSY contributions in the code `FeynHiggs` as described in Ref. [184].

Concerning the prediction for M_W in the SM, the central value of $M_W^{\rm SM}$ quoted in Eq. (5) (which agrees with the result obtained from the fit formula in Ref. [49] within the theoretical uncertainty) has been obtained for the following input parameters:

$$\begin{aligned}
&\alpha(0)^{-1} = 137.035999084, \quad M_Z = 91.1876\ \text{GeV},\\
&G_F = 1.166378 \cdot 10^{-5}\ \text{GeV}^{-2},\\
&\Delta\alpha_{\rm had}^{(5)}(M_Z) = 0.02766, \quad m_t = 172.76\ \text{GeV},\\
&M_H^{\rm SM} = 125.09\,\text{GeV},\\
&\Delta\alpha_{\rm lept} = 0.031497686, \quad m_b(m_b) = 4.18\ \text{GeV},\\
&\alpha_s(M_Z) = 0.1179.
\end{aligned} \tag{7}$$

All these values are from Ref. [45], except for $\Delta\alpha_{\rm lept}$, which is taken from Ref. [185]. Besides the "intrinsic" theoretical uncertainties from unknown higher-order corrections, see the estimate in Eq. (5) for the SM, the predictions in the SM and the MSSM are also affected by theoretical uncertainties that are induced by the experimental errors of the input parameters. For the SM case the latter "parametric" uncertainties can be estimated by recomputing $M_W^{\rm SM}$ for numerical values of the input parameters that are shifted with respect to the ones quoted in Eq. (7) by their experimental errors (where we use the values given in Ref. [45] unless otherwise specified): for the case of the top-quark mass, m_t, a variation of ± 1 GeV [4] changes $M_W^{\rm SM}$ by $\pm\,6$ MeV; a shift of $\pm\,0.0010$ from the central value $\alpha_s(M_Z)$ yields a variation of ± 0.7 MeV in $M_W^{\rm SM}$; the uncertainty on M_Z is of $\pm\,0.0021$ GeV and its impact on $M_W^{\rm SM}$ is of $\simeq \pm\,2.7$ MeV; the uncertainty of 0.00007 on the value of $\Delta\alpha_{\rm had}^{(5)}(M_Z)$ yields a variation of $\simeq$ 1.2 MeV; finally, varying the Higgs mass by 1 GeV results in a shift of $\simeq$ 0.4 MeV.

[2] See e.g. Ref. [147] for the case of a model where the lowest-order prediction for M_W is modified.

[3] See also Refs. [176–179] for further higher-order contributions involving fermion loops.

[4] This value is indicated for illustration. The parametric uncertainty of the top-quark mass has to be assessed on the basis of the experimental error of the measured mass parameter of ± 0.30 GeV at the 1 σ level [45] in combination with the systematic uncertainty that is associated with relating the measured quantity to a theoretically well-defined top-quark mass.

Concerning the theoretical uncertainties of the MSSM prediction for M_W, our implementation described above is such that in the decoupling limit the intrinsic and parametric theoretical uncertainties of the M_W prediction are the same as for the SM case. If some of the SUSY particles are relatively light the intrinsic theoretical uncertainties can be somewhat larger, depending on the mass scales of the SUSY parameters, see, e.g., the discussion in Ref. [53]. The sensitivity of the M_W prediction to variations of the SUSY parameters is usually not discussed as a parametric uncertainty, but as an indication of the sensitivity of a precise measurement of M_W for constraining the allowed range of SUSY parameters. In our numerical analysis below the intrinsic theoretical uncertainty of the prediction for M_W in the MSSM from unknown higher-order corrections and the parametric uncertainty from varying the SM input parameters will not be displayed. On the other hand, we also show for comparison the SM prediction, where the current intrinsic theoretical uncertainty from unknown higher-order corrections of ± 4 MeV, see Eq. (5), is indicated as a horizontal band.

We furthermore indicate in our plots below the current experimental value for M_W and its $\pm 1\sigma$ band as given in Eq. (4). For illustration also a projected future uncertainty that can be expected at the ILC of $\delta M_W^{\rm ILC} = 0.003$ GeV [186] is shown. In principle an even higher precision of $\mathcal{O}(1$ MeV) could be achieved at the FCC-ee [187,188] or at the CEPC [189,190], but in the projections that were carried out theory uncertainties affecting the measurement were not taken into account. Those theoretical uncertainties may give rise to a systematic experimental uncertainty that dominates over the expected statistical uncertainty [51,52].

2.4 Parameter scan

We use the parameter sets that were obtained in Refs. [33–35] from a scan of the EW MSSM parameter space making use of the code `SuSpect-2.43` [191]. The applied constraints discussed above, in particular the compatibility with Δa_μ as given in Eq. (3) at the $2\,\sigma$ level and with the upper bound on the DM relic density, give rise to lower and upper limits on the relevant neutralino, chargino and slepton masses. As detailed in Refs. [33,34] five scan regions cover the relevant parameter space:

(A) Mixed bino/wino DM with $\tilde\chi_1^\pm$-coannihilation

$$\begin{aligned} &100\ \text{GeV} \le M_1 \le 1\ \text{TeV}, \quad M_1 \le M_2 \le 1.1 M_1, \\ &1.1 M_1 \le \mu \le 10 M_1, \quad 5 \le \tan\beta \le 60, \\ &100\ \text{GeV} \le m_{\tilde l_L} \le 1\ \text{TeV}, \quad m_{\tilde l_R} = m_{\tilde l_L}\ . \end{aligned} \tag{8}$$

Bino DM with $\tilde l^\pm$-coannihilation region

(B) Case-L: SU(2) doublet

$$\begin{aligned} &100\ \text{GeV} \le M_1 \le 1\ \text{TeV}, \quad M_1 \le M_2 \le 10 M_1, \\ &1.1 M_1 \le \mu \le 10 M_1, \quad 5 \le \tan\beta \le 60, \\ &M_1 \le m_{\tilde l_L} \le 1.2 M_1, \quad M_1 \le m_{\tilde l_R} \le 10 M_1\ . \end{aligned} \tag{9}$$

(C) Case-R: SU(2) singlet

$$\begin{aligned} &100\ \text{GeV} \le M_1 \le 1\ \text{TeV}, \quad M_1 \le M_2 \le 10 M_1, \\ &1.1 M_1 \le \mu \le 10 M_1, \quad 5 \le \tan\beta \le 60, \\ &M_1 \le m_{\tilde l_R} \le 1.2 M_1, \quad M_1 \le m_{\tilde l_L} \le 10 M_1\ . \end{aligned} \tag{10}$$

(D) Higgsino DM

$$\begin{aligned} &100\ \text{GeV} \le \mu \le 1.2\ \text{TeV}, \quad 1.1\mu \le M_1 \le 10\mu, \\ &1.1\mu \le M_2 \le 10\mu, \quad 5 \le \tan\beta \le 60, \\ &100\ \text{GeV} \le m_{\tilde l_L}, m_{\tilde l_R} \le 2\ \text{TeV}. \end{aligned} \tag{11}$$

(E) Wino DM

$$\begin{aligned} &100\ \text{GeV} \le M_2 \le 1.5\ \text{TeV}, \quad 1.1 M_2 \le M_1 \le 10 M_2, \\ &1.1 M_2 \le \mu \le 10 M_2, \quad 5 \le \tan\beta \le 60, \\ &100\ \text{GeV} \le m_{\tilde l_L}, m_{\tilde l_R} \le 2\ \text{TeV}. \end{aligned} \tag{12}$$

For each of the five scenarios a data sample of $\mathcal{O}(10^7)$ points was generated by scanning randomly over the input parameter ranges specified above, using a flat prior for all parameters. Since we have assumed the colored SUSY sector to be heavy, the parameters of the squark and gluino sectors are not varied in the scan (see above for the prescription that was used for obtaining a prediction for the mass of the SM-like Higgs boson that is in agreement with the experimental result). We have checked for our scan points that the contribution from colored SUSY particles to $M_W^{\rm MSSM}$ is indeed negligible.

3 Results

In the following we present the results for the scan points that are allowed by the experimental and theoretical constraints specified in Sect. 2.2 in the five scenarios defined above. In particular, the displayed scan points are in agreement with Δa_μ, as given in Eq. (3), at the 1 and $2\,\sigma$ level.

In Fig. 1 we show in the $\Delta a_\mu^{\rm MSSM}$–M_W plane the results for the five scenarios corresponding to the $\tilde l^\pm$-coannihilation case-L and case-R, the $\tilde\chi_1^\pm$-coannihilation case, the wino and the higgsino case. The prediction for $\Delta a_\mu^{\rm MSSM}$ has been evaluated with the code `GM2Calc-1.7.5` [138]. The vertical solid blue line indicates the value of Δa_μ as given in Eq. (3), while its $\pm 1\,\sigma$ range is indicated by the blue dashed vertical lines. The displayed points are restricted to the $\pm 2\,\sigma$ range of Δa_μ. The horizontal lines indicate the current central value for $M_W^{\rm exp}$ (solid green), the current $\pm 1\,\sigma$ uncertainties (green

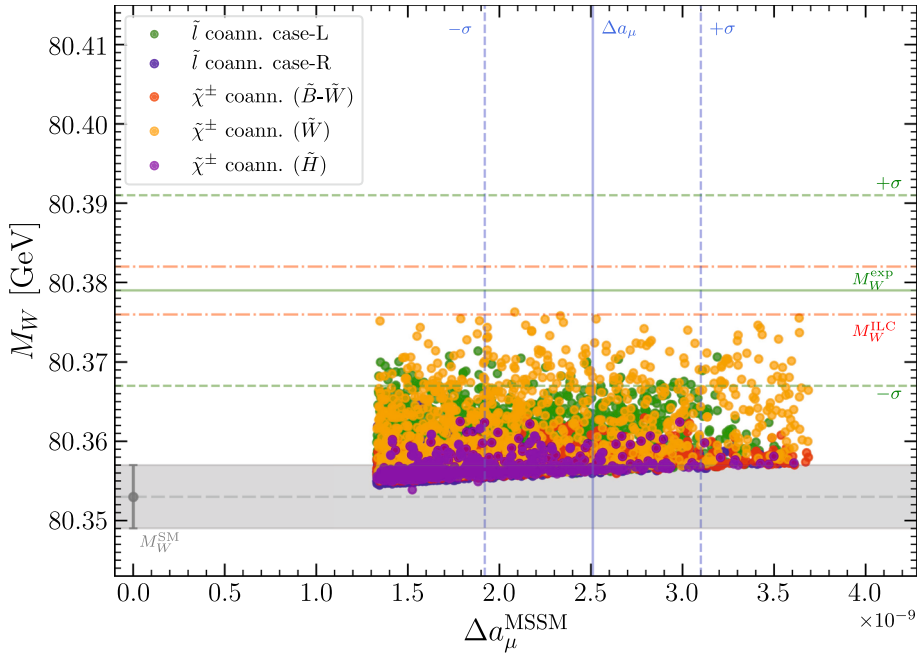

Fig. 1 Results for the five considered scenarios in the $\Delta a_\mu^{\rm MSSM}$–M_W plane, where the prediction for $\Delta a_\mu^{\rm MSSM}$ has been evaluated with the code `GM2Calc-1.7.5` [138]. The points for the $\tilde{l}^{\pm}$-coannihilation case-L and case-R, the $\tilde{\chi}_1^{\pm}$-coannihilation case, the wino and the higgsino case are shown in green, blue, red, orange and violet, respectively. The vertical blue lines indicate the central value of Δa_μ as given in Eq. (3) (solid) and its $\pm 1\,\sigma$ range (dashed). The displayed points are restricted to the $\pm 2\,\sigma$ range of Δa_μ. The horizontal lines indicate the current central value for $M_W^{\rm exp}$ (solid green), the current $\pm 1\,\sigma$ uncertainties (green dashed) and the anticipated ILC $\pm 1\,\sigma$ (red dot-dashed) uncertainties. The SM prediction is shown as a point for $\Delta a_\mu^{\rm MSSM} = 0$, while the gray band indicates the theoretical uncertainty of the SM prediction for M_W from unknown higher-order corrections

dashed) and the anticipated ILC $\pm 1\,\sigma$ (red shaded) uncertainties. The SM prediction is shown in gray, including the theoretical uncertainty from unknown higher-order corrections.

One can observe in all scenarios a lower limit on $M_W^{\rm MSSM}$ that for small $\Delta a_\mu^{\rm MSSM}$, corresponding to heavy EW SUSY masses, recovers the SM prediction (within $\sim$ 1 MeV; this offset would be absent for even smaller values of $\Delta a_\mu^{\rm MSSM}$). The lower limit rises for increasing $\Delta a_\mu^{\rm MSSM}$ by up to $\sim$ 3 MeV. Thus, the relatively light SUSY particles that are required for larger values of $\Delta a_\mu^{\rm MSSM}$ give rise to a slight increase in the prediction for M_W that is independent of the variation of the other parameters in the scan. While this lower limit on the predicted value of M_W is very similar in the five DM scenarios, there are important differences in the highest $M_W^{\rm MSSM}$ values that are reached. The largest predicted values of $M_W^{\rm MSSM}$, nearly reaching the current central value of $M_W^{\rm exp}$, are obtained for the wino DM case. Accordingly, for the wino DM case the electroweak sector of the MSSM behaves in such a way that the predicted values for M_W and the anomalous magnetic moment of the muon can simultaneously be very close to the present experimental central values, while respecting all other constraints on the model. For the $\tilde{l}^{\pm}$-coannihilation case-L the highest obtained $M_W^{\rm MSSM}$ values are somewhat lower but still within the current $\pm\,1\,\sigma$ range of $M_W^{\rm exp}$. On the other hand, for the other three scenarios we find significantly lower predicted values of M_W.

These results open interesting perspectives for discriminating between different DM scenarios with the anticipated future accuracy on M_W. Depending of course on the future central value of M_W, the wino DM scenario could potentially be singled out as the only scenario yielding a good agreement with the M_W measurement. As we will discuss in more detail below, an $M_W^{\rm MSSM}$ prediction near the current experimental central value implies that at least some of the SUSY particles have to be relatively light, offering good prospects for the SUSY searches at the LHC and future colliders. If instead the future central value of $M_W^{\rm exp}$ turns out to be substantially lower, outside of the current $\pm 1\,\sigma$ range, all the considered DM scenarios could still be in agreement with the M_W measurement. On the other hand, a higher central value of $M_W^{\rm exp}$ would require larger contributions from the EW SUSY states, possibly via further relaxed assumptions on the EW SUSY parameters, or additional contributions from the colored sector (as discussed above, the latter possibility is not considered in the present study).

In Fig. 2 we analyze in more detail the origin of the contributions to $M_W^{\rm MSSM}$. We show the M_W prediction as a function

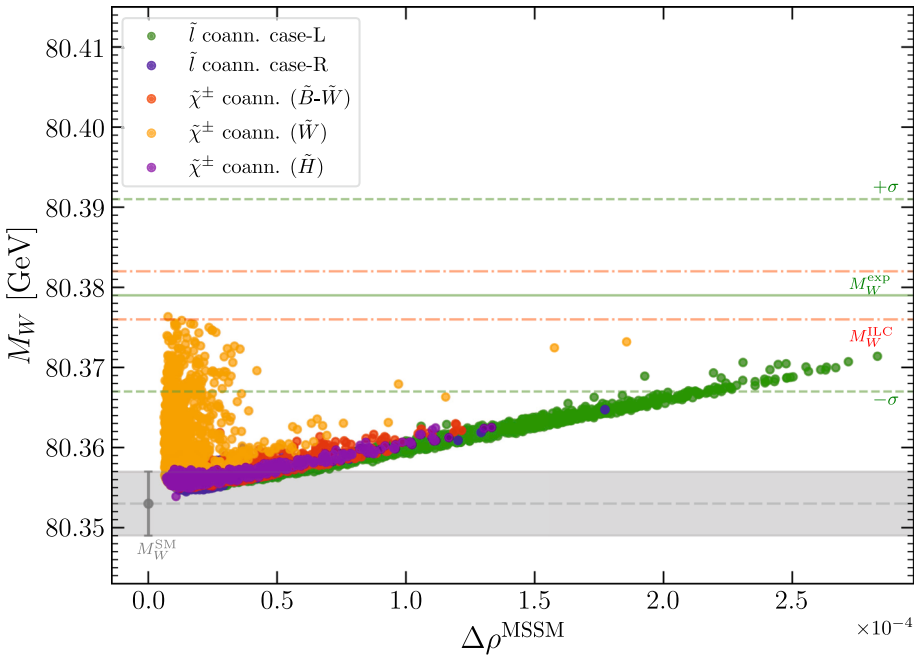

Fig. 2 Results for the five scenarios in the $\Delta\rho^{\rm MSSM}$–M_W plane. The horizontal lines and the color coding are as in Fig. 1

of $\Delta\rho^{\rm MSSM}$, which denotes the SUSY contributions from sfermions to the quantity $\Delta\rho$. As discussed above, the contribution of pure slepton loops enters only via self-energies, and in particular via the SUSY contributions to $\Delta\rho$. On the other hand, "mixed" slepton/chargino/neutralino contributions enter via the vertex and box corrections to Δr. One can see in Fig. 2 that the largest corrections to $M_W^{\rm MSSM}$ that were found for wino DM and the $\tilde{l}^{\pm}$-coannihilation case-L in Fig. 1 have different origins. Wino DM, which naturally has at least one light neutralino and one light chargino in the spectrum, can yield sizable contributions to $M_W^{\rm MSSM}$ even for small $\Delta\rho^{\rm MSSM}$. On the other hand, for $\tilde{l}^{\pm}$-coannihilation, which naturally has light sleptons in the spectrum, large corrections to $M_W^{\rm MSSM}$ are correlated with large contributions of $\Delta\rho$, while the vertex and box contributions in this case are sub-dominant. We have explicitly verified these features by enabling and disabling the respective contributions in the $M_W^{\rm MSSM}$ calculation.

Consequently, in the following we discuss the dependence of $M_W^{\rm MSSM}$ on the various SUSY particle masses. We will focus our discussion on the two scenarios that show an appreciable contribution to $M_W^{\rm MSSM}$, wino DM and the $\tilde{l}^{\pm}$-coannihilation case-L. For the other scenarios the impact of an improved accuracy of the M_W measurement on the parameter space can be summarized as follows: for an experimental central value that is close to the SM prediction the discriminating power between different SUSY scenarios will be limited; on the other hand, if the experimental central value stays close to the current value those scenarios will be disfavored by the M_W measurement (unless relatively light colored particles would yield an upward shift in the M_W prediction).

We start our discussion of the SUSY mass dependences of $M_W^{\rm MSSM}$ in Fig. 3 with the prediction of the W-boson mass as a function of $m_{\tilde{\chi}_1^0}$. In our scan we find values of the LSP mass between $\sim$ 100 GeV and up to $\sim$ 600 GeV, where the specific values depend on the scenario (see also the discussion in Refs. [33–36]). In particular, only for $\tilde{l}^{\pm}$-coannihilation and wino DM very low values of $m_{\tilde{\chi}_1^0}$ are realized. The large contributions to $M_W^{\rm MSSM}$ in the wino DM scenario and for the $\tilde{l}^{\pm}$-coannihilation case-L are reached only for $m_{\tilde{\chi}_1^0} \lesssim 150$ GeV. For larger LSP masses the MSSM prediction for M_W approaches the SM limit, indicating a decoupling effect of the SUSY contributions. The low $m_{\tilde{\chi}_1^0}$ values that can bring the M_W prediction close to the experimental central value provide an interesting target that can be probed via SUSY searches at the LHC and future colliders.

In Fig. 4 we show the dependence of $M_W^{\rm MSSM}$ on the lightest chargino mass, $m_{\tilde{\chi}_1^{\pm}}$. The largest contributions to $M_W^{\rm MSSM}$ are obtained for the smallest chargino masses, $m_{\tilde{\chi}_1^{\pm}} \lesssim 200$ GeV. On the other hand, for the $\tilde{l}^{\pm}$-coannihilation case-L M_W values within the current $1\,\sigma$ bound are reached for masses up to $m_{\tilde{\chi}_1^{\pm}} \lesssim 800$ GeV. The visible "hole" in this scenario for 200 GeV $\lesssim m_{\tilde{\chi}_1^{\pm}} \lesssim$ 350 GeV, where no scan points passed the applied constraints, is due to the experimental constraints from the LHC. In particular, the strongest impact comes from the ATLAS $3l+\not{E}_T$ search [192], which is sensitive to the production of a pair of $\tilde{\chi}_1^{\pm}\tilde{\chi}_2^0$ with subsequent decay via sleptons.

Next, in Figs. 5 and 6 we show the dependence of the $M_W^{\rm MSSM}$ prediction on $m_{\tilde{\mu}_L}$ and $m_{\tilde{\mu}_R}$, respectively. For the $\tilde{l}^{\pm}$-coannihilation case-L naturally a light $\tilde{\mu}_L$ is present in the particle spectrum, close in mass to the LSP, as can be

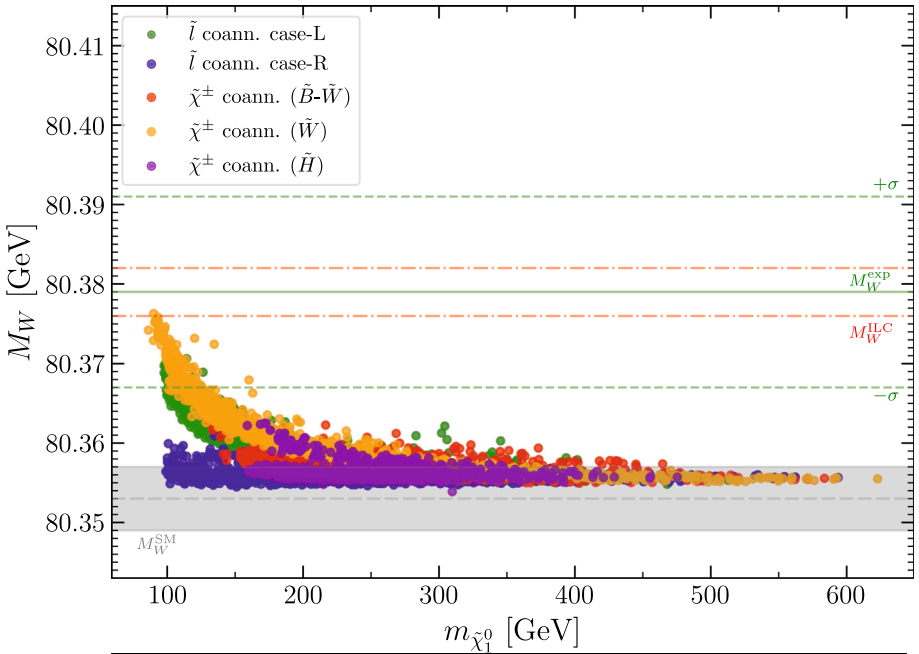

Fig. 3 Results for the five scenarios in the $m_{\tilde{\chi}_1^0}$–M_W plane. The horizontal lines and the color coding are as in Fig. 1

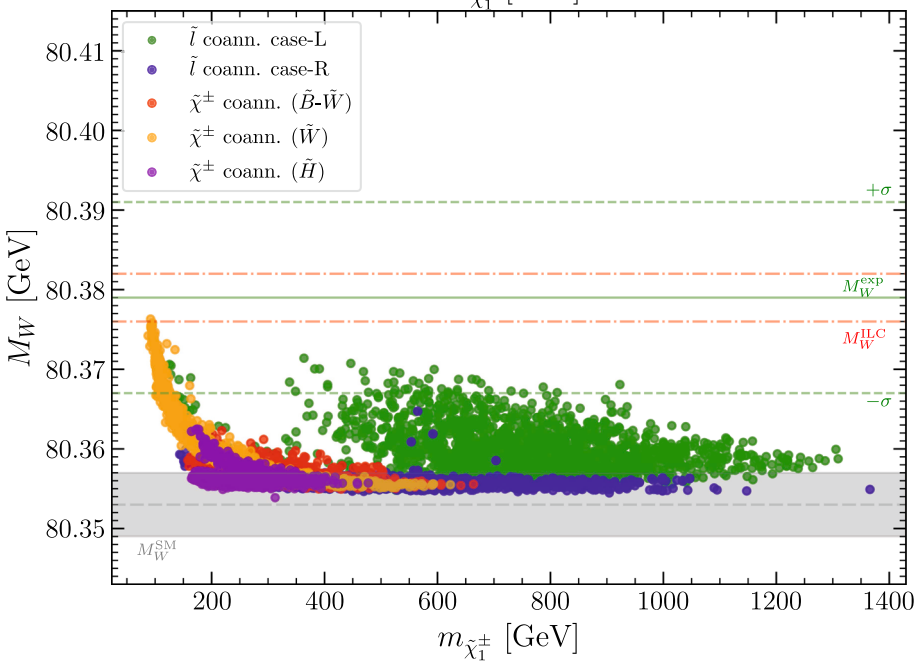

Fig. 4 Results for the five scenarios in the $m_{\tilde{\chi}_1^{\pm}}$–M_W plane. The horizontal lines and the color coding are as in Fig. 1

seen in Fig. 5. Consequently, see Fig. 3, the largest contributions to $M_W^{\rm MSSM}$ are reached for the lowest values of $m_{\tilde{\mu}_L}$. Thus, the low values of $\tilde{\mu}_L$ that are required in this scenario in order to bring the M_W prediction close to the experimental central value offer interesting prospects for upcoming searches for SUSY particles. The case is different for wino DM. Here $M_W^{\rm MSSM}$ values within the $1\,\sigma$ interval of $M_W^{\rm exp}$ are reached for 200 GeV $\lesssim m_{\tilde{\mu}_L} \lesssim$ 1200 GeV, which will make it difficult to conclusively probe this scenario at the HL-LHC or the ILC, see also the discussion in Refs. [33–35]. Clearly visible is also a "hole" in the $m_{\tilde{\mu}_L}$ parameter space at 250 GeV $\lesssim m_{\tilde{\mu}_L} \lesssim$ 400 GeV, where no scan points are allowed by the applied constraints. We found that this is due to the experimental constraints from the LHC, specifically from slepton pair production searches in the 2l+$\not{E}_T$ channel [193].

As shown in Fig. 6, for the wino DM scenario an M_W prediction close to the experimental central value is correlated with a similar range of $\tilde{\mu}_R$ values as it was the case for $\tilde{\mu}_L$ in Fig. 5. On the other hand, for the $\tilde{l}^{\pm}$-coannihilation case-L scenario the M_W prediction is only weakly sensitive on $\tilde{\mu}_R$ in contrast to the case of $\tilde{\mu}_L$. Values of $M_W^{\rm MSSM}$ within the $1\,\sigma$ experimental limit are reached for the whole range of 200 GeV $\lesssim m_{\tilde{\mu}_R} \lesssim$ 1300 GeV.

As final step of our analysis we show in Fig. 7 the dependence of $M_W^{\rm MSSM}$ on $\tan\beta$. In Refs. [33–35] it was shown

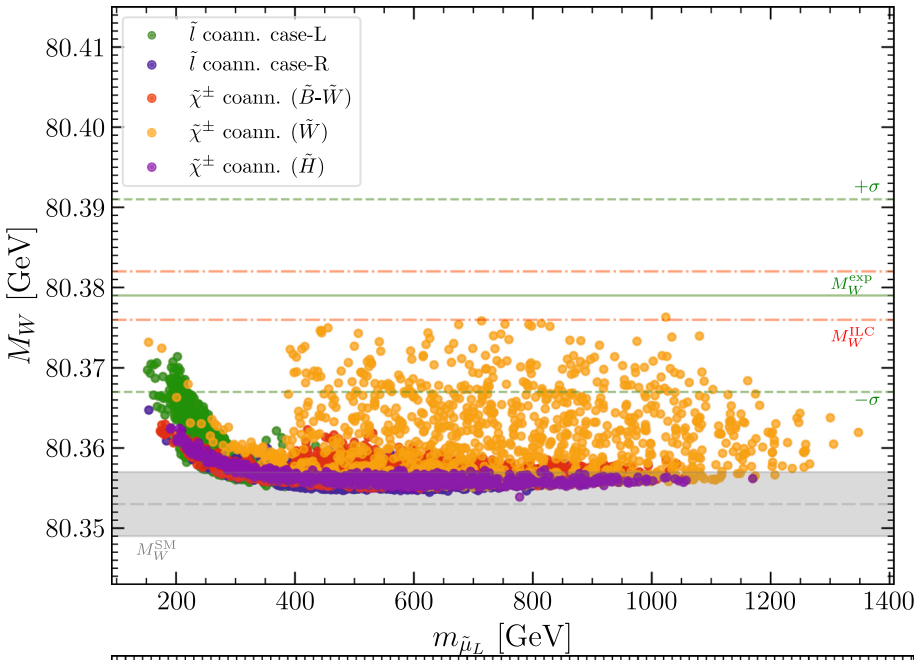

Fig. 5 Results for the five scenarios in the $m_{\tilde{\mu}_L}$–M_W plane. The horizontal lines and the color coding are as in Fig. 1

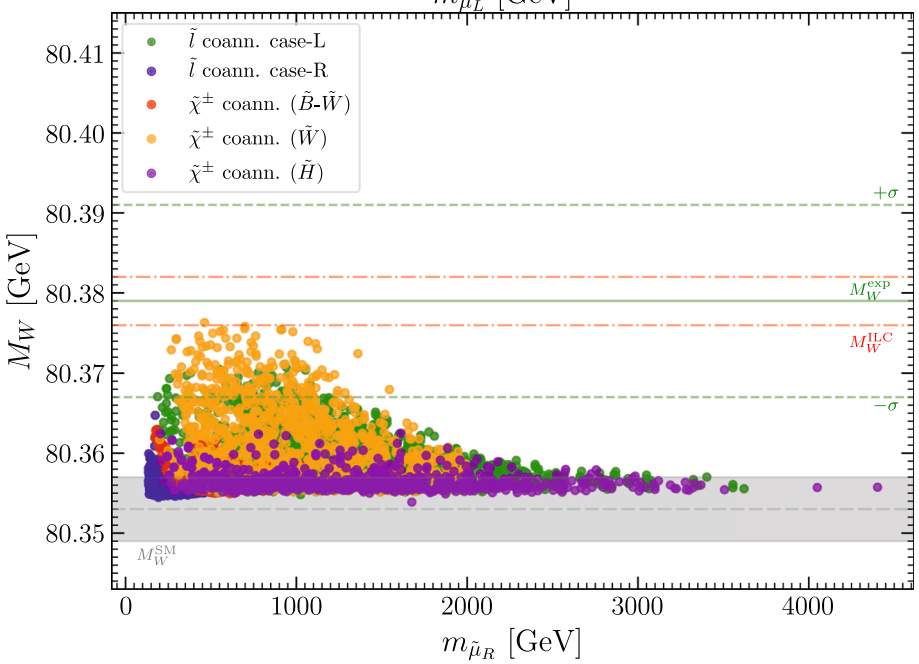

Fig. 6 Results for the five scenarios in the $m_{\tilde{\mu}_R}$–M_W plane. The horizontal lines and the color coding are as in Fig. 1

that low values of $m_{\tilde{\chi}_1^0}$ can yield a prediction for $a_\mu^{\rm MSSM}$ in the preferred region for effectively the whole allowed $\tan\beta$ range. Consequently, no pronounced dependence of $M_W^{\rm MSSM}$ on $\tan\beta$ is expected, see also Refs. [53,55]. This is confirmed in Fig. 7. Values of $M_W^{\rm MSSM}$ in the experimental $1\,\sigma$ range are found for $5 \lesssim \tan\beta \lesssim 60(50)$ for the wino DM ($\tilde{l}^{\pm}$-coannihilation case-L) scenario.

4 Conclusions and outlook

The new result for the Run 1 data of the "MUON G-2" experiment confirmed the deviation from the SM prediction found previously. The combination of the experimental results yields a discrepancy with the theory world average for the SM prediction of $\Delta a_\mu = (25.1 \pm 5.9) \times 10^{-10}$, corresponding to a $4.2\,\sigma$ effect. Contributions from the EW sector of the MSSM, consisting of charginos, neutralinos and scalar leptons, can bring the theoretical prediction into very good agreement with the new combined average of $a_\mu^{\rm exp}$, while at the same time complying with all other experimental and theoretical constraints on this sector. In particular, identifying the lightest neutralino, $\tilde{\chi}_1^0$, with the LSP, a prediction for the CDM relic abundance can be obtained that is in accordance with the experimental observation, while respecting

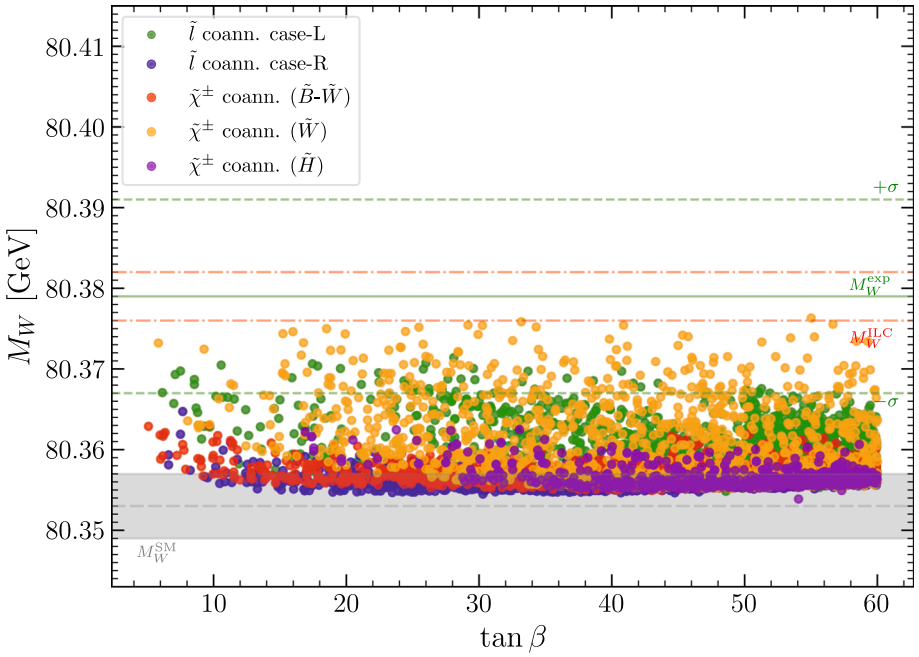

Fig. 7 Results for the five scenarios in the tan β–M_W plane. The horizontal lines and the color coding are as in Fig. 1

the bounds from DM direct detection experiments as well as from direct searches for new particles at the LHC.

Using the Planck measurement of the DM relic density as an upper limit on the DM content that is associated with $\tilde{\chi}_1^0$, we analyzed the prediction for the W-boson mass in the MSSM, $M_W^{\rm MSSM}$. We assumed that the colored sector of the MSSM is heavy such that it is in agreement with the LHC limits from direct searches for SUSY particles and at the same time yields a negligible contribution to $M_W^{\rm MSSM}$. In general, the direct search limits in combination with the requirement to obtain a prediction for M_h that within the theoretical uncertainties is in agreement with the measured mass value of the SM-like Higgs boson of about 125 GeV yields a lower bound on the scale of the stop masses of $\gtrsim$ 1–1.5 TeV. While the squark contributions to $M_W^{\rm MSSM}$ tend to be relatively small in this mass region, they are not necessarily negligible if the third generation squark masses happen to be close to this lower bound and/or if large mixing is present. We have checked the numerical impact of those contributions and found that an upward shift of $M_W^{\rm MSSM}$ of about 20 MeV or more is possible for the case of the parameter sets in this study where the stop and sbottom masses are near 1.5 TeV and the constraint on M_h is satisfied, see also the discussion in Ref. [55]. Accordingly, an analysis targeting the lowest possible mass values of the third generation squarks in the MSSM should take into account also the contribution of the colored sector to $M_W^{\rm MSSM}$. We leave such an investigation for future work.

We analyzed five scenarios, depending on the mechanism that brings the relic density in agreement with the observed upper bound: bino/wino DM with $\tilde{\chi}_1^{\pm}$-coannihilation, bino DM with $\tilde{l}^{\pm}$-coannihilation with the mass of the "left-handed" ("right-handed") slepton close to $m_{\tilde{\chi}_1^0}$, case-L (case-R), wino DM and higgsino DM. We find that only the scenarios of wino DM and the $\tilde{l}^{\pm}$-coannihilation case-L can give rise to sizable contributions to $M_W^{\rm MSSM}$, up to $\sim$ 25 MeV and $\sim$ 20 MeV, respectively. Accordingly, in those scenarios the predicted values for M_W and a_μ can simultaneously be very close to the present experimental central values. As a consequence, the anticipated future accuracy on M_W offers interesting prospects for discriminating between different DM scenarios, depending on the future experimental central value for M_W.

For the $\tilde{l}^{\pm}$-coannihilation case-L the numerically important corrections stem mostly from the self-energy contributions, whereas for wino DM the vertex and box contributions are most relevant. In these scenarios the largest $M_W^{\rm MSSM}$ values are reached for the smallest experimentally allowed $\tilde{\chi}_1^0$ masses, $m_{\tilde{\chi}_1^0} \lesssim 150$ GeV. Concerning the other EW SUSY masses, sizable contributions to $M_W^{\rm MSSM}$ require a light chargino, $m_{\tilde{\chi}_1^{\pm}} \lesssim 200$ GeV for wino DM, or a light "left-handed" smuon, $m_{\tilde{\mu}_L} \lesssim 250$ GeV for the $\tilde{l}^{\pm}$-coannihilation case-L. The combined analysis of a_μ, M_W and the DM relic density therefore leads to preferred mass regions of the specified SUSY states that can serve as targets for searches at the (HL-)LHC and future e^+e^- colliders, such as the "second stage" ILC with $\sqrt{s} = 500$ GeV.

The complementary information from future searches for new particles and from an increased sensitivity of the precision observables a_μ and M_W will give rise to stringent tests of the theory of the electroweak interactions. We have indicated in our plots the prospective improvement on the precision for $M_W^{\rm exp}$, displayed for the example of the expected accuracy at the ILC, $\delta M_W^{\rm ILC} \sim 3$ MeV. If the future central value of $M_W^{\rm exp}$

stays close to the present value, the SM would be strongly disfavored, and also various MSSM scenarios would yield a large discrepancy between the theory prediction and the experimental value of M_W. On the other hand, the scenarios with light EW SUSY particles yielding predictions of a_μ and M_W close to the current experimental central values would clearly offer very good prospects for future e^+e^- colliders.

Note added

Shortly after submission of this paper a new measurement of M_W was reported by the CDF collaboration [194], corresponding to $M_W^{\mathrm{CDF-new}} = 80.4335 \pm 0.0094$ GeV, which lies substantially above the experimental PDG average, Eq. (4). The main emphasis of this article is the correlation between the EW SUSY sector giving a good description for $(g-2)_\mu$ and the corresponding effects on the M_W prediction from these EW particles, focusing on the current PDG value of M_W^{exp} (no new official average including the recent CDF measurement is available so far). In the future it will be mandatory to assess the compatibility of the different measurements of M_W and to carefully analyze possible sources of systematic effects. However, if an experimental value substantially above the current PDG value (as indicated by the new CDF measurement) is confirmed, an analysis including the effects of SU(2) breaking in the stop/sbottom sector will be necessary, as discussed in Sect. 4.

Acknowledgements We thank M. Berger, M. Falck and G. Moortgat-Pick for useful discussions. The work of I.S. is supported by World Premier International Research Center Initiative (WPI), MEXT, Japan. The work of S. H. is supported in part by the Grant PID2019-110058GB-C21 funded by MCIN/AEI/10.13039/501100011033 and by "ERDF A way of making Europe", and in part by the Grant CEX2020-001007-S funded by MCIN/AEI/10.13039/501100011033. The work of M.C. is supported by the project AstroCeNT: Particle Astrophysics Science and Technology Centre, carried out within the International Research Agendas programme of the Foundation for Polish Science financed by the European Union under the European Regional Development Fund. G. W. acknowledges support by the Deutsche Forschungsgemeinschaft (DFG, German Research Foundation) under Germany's Excellence Strategy—EXC 2121 "Quantum Universe"—390833306. This work has been partially funded by the Deutsche Forschungsgemeinschaft (DFG, German Research Foundation)—491245950.

Data Availability Statement This manuscript has no associated data or the data will not be deposited. [Authors' comment: This is a theoretical study and no experimental data has been generated or used, aside from the results of measurements already publicly released by the experimental collaborations.]

Funded by SCOAP[3].

References

1. J. Grange et al. [Muon g-2 Collaboration], arXiv:1501.06858 [physics.ins-det]
2. B. Abi et al. [Muon g-2], Phys. Rev. Lett. **126**(14), 141801 (2021). arXiv:2104.03281 [hep-ex]
3. T. Aoyama et al., Phys. Rep. **887**, 1–166 (2020). arXiv:2006.04822 [hep-ph]
4. T. Aoyama, M. Hayakawa, T. Kinoshita, M. Nio, Phys. Rev. Lett. **109**, 111808 (2012). arXiv:1205.5370 [hep-ph]
5. T. Aoyama, T. Kinoshita, M. Nio, Atoms **7**(1), 28 (2019)
6. A. Czarnecki, W.J. Marciano, A. Vainshtein, Phys. Rev. D **67**, 073006 (2003). arXiv:hep-ph/0212229
7. C. Gnendiger, D. Stöckinger, H. Stöckinger-Kim, Phys. Rev. D **88**, 053005 (2013). arXiv:1306.5546 [hep-ph]
8. M. Davier, A. Hoecker, B. Malaescu, Z. Zhang, Eur. Phys. J. C **77**(12), 827 (2017). arXiv:1706.09436
9. A. Keshavarzi, D. Nomura, T. Teubner, Phys. Rev. D **97**(11), 114025 (2018). arXiv:1802.02995 [hep-ph]
10. G. Colangelo, M. Hoferichter, P. Stoffer, JHEP **02**, 006 (2019). arXiv:1810.00007 [hep-ph]
11. M. Hoferichter, B.L. Hoid, B. Kubis, JHEP **08**, 137 (2019). arXiv:1907.01556 [hep-ph]
12. M. Davier, A. Hoecker, B. Malaescu, Z. Zhang, Eur. Phys. J. C **80**(3), 241 (2020). arXiv:1908.00921 [hep-ph]
13. A. Keshavarzi, D. Nomura, T. Teubner, Phys. Rev. D **101**(1), 014029 (2020). arXiv:1911.00367 [hep-ph]
14. A. Kurz, T. Liu, P. Marquard, M. Steinhauser, Phys. Lett. B **734**, 144–147 (2014). arXiv:1403.6400 [hep-ph]
15. K. Melnikov, A. Vainshtein, Phys. Rev. D **70**, 113006 (2004). arXiv:hep-ph/0312226
16. P. Masjuan, P. Sanchez-Puertas, Phys. Rev. D **95**(5), 054026 (2017). arXiv:1701.05829 [hep-ph]
17. G. Colangelo, M. Hoferichter, M. Procura, P. Stoffer, JHEP **04**, 161 (2017). arXiv:1702.07347 [hep-ph]
18. M. Hoferichter, B.L. Hoid, B. Kubis, S. Leupold, S.P. Schneider, JHEP **10**, 141 (2018). arXiv:1808.04823 [hep-ph]
19. A. Gérardin, H.B. Meyer, A. Nyffeler, Phys. Rev. D **100**(3), 034520 (2019). arXiv:1903.09471 [hep-lat]
20. J. Bijnens, N. Hermansson-Truedsson, A. Rodríguez-Sánchez, Phys. Lett. B **798**, 134994 (2019). arXiv:1908.03331 [hep-ph]
21. G. Colangelo, F. Hagelstein, M. Hoferichter, L. Laub, P. Stoffer, JHEP **03**, 101 (2020). arXiv:1910.13432 [hep-ph]
22. T. Blum, N. Christ, M. Hayakawa, T. Izubuchi, L. Jin, C. Jung, C. Lehner, Phys. Rev. Lett. **124**(13), 132002 (2020). arXiv:1911.08123 [hep-lat]
23. G. Colangelo, M. Hoferichter, A. Nyffeler, M. Passera, P. Stoffer, Phys. Lett. B **735**, 90–91 (2014). arXiv:1403.7512 [hep-ph]
24. S. Borsanyi et al., Nature **593**(7857), 51–55 (2021). arXiv:2002.12347 [hep-lat]
25. C. Lehner, A.S. Meyer, Phys. Rev. D **101**, 074515 (2020). arXiv:2003.04177 [hep-at]
26. E. de Rafael, Phys. Rev. D **102**(5), 056025 (2020). arXiv:2006.13880 [hep-ph]
27. A. Crivellin, M. Hoferichter, C.A. Manzari, M. Montull, Phys. Rev. Lett. **125**(9), 091801 (2020). arXiv:2003.04886 [hep-ph]

28. A. Keshavarzi, W.J. Marciano, M. Passera, A. Sirlin, Phys. Rev. D **102**(3), 033002 (2020). arXiv:2006.12666 [hep-ph]
29. H. Nilles, Phys. Rep. **110**, 1 (1984)
30. R. Barbieri, Riv. Nuovo Cim. **11**, 1 (1988)
31. H. Haber, G. Kane, Phys. Rep. **117**, 75 (1985)
32. J. Gunion, H. Haber, Nucl. Phys. B **272**, 1 (1986)
33. M. Chakraborti, S. Heinemeyer, I. Saha, Eur. Phys. J. C **80**(10), 984 (2020). arXiv:2006.15157 [hep-ph]
34. M. Chakraborti, S. Heinemeyer, I. Saha, Eur. Phys. J. C **81**(12), 1069 (2021). arXiv:2103.13403 [hep-ph]
35. M. Chakraborti, S. Heinemeyer, I. Saha, Eur. Phys. J. C **81**(12), 1114 (2021). arXiv:2104.03287 [hep-ph]
36. M. Chakraborti, S. Heinemeyer, I. Saha, C. Schappacher, arXiv:2112.01389 [hep-ph]
37. H. Goldberg, Phys. Rev. Lett. **50**, 1419 (1983)
38. J. Ellis, J. Hagelin, D. Nanopoulos, K. Olive, M. Srednicki, Nucl. Phys. B **238**, 453 (1984)
39. See:https://twiki.cern.ch/twiki/bin/view/AtlasPublic/SupersymmetryPublicResults
40. See:https://twiki.cern.ch/twiki/bin/view/CMSPublic/PhysicsResultsSUS
41. N. Aghanim et al. [Planck], Astron. Astrophys. **641** (2020), A6. arXiv:1807.06209 [astro-ph.CO] [Erratum: *Astron. Astrophys.* **652** (2021), C4]
42. E. Aprile et al. [XENON Collaboration], Phys. Rev. Lett. **121**(11), 111302 (2018) arXiv:1805.12562 [astro-ph.CO]
43. D.S. Akerib et al. [LUX Collaboration], Phys. Rev. Lett. **118**(2), 021303 (2017). arXiv:1608.07648 [astro-ph.CO]
44. X. Cui et al. [PandaX-II Collaboration], Phys. Rev. Lett. **119**(18), 181302 (2017). arXiv:1708.06917 [astro-ph.CO]
45. P.A. Zyla et al. [Particle Data Group], PTEP **2020**(8), 083C01 (2020)
46. S. Heinemeyer, W. Hollik, G. Weiglein, Comput. Phys. Commun. **124**, 76 (2000). arXiv:hep-ph/9812320
47. T. Hahn, S. Heinemeyer, W. Hollik, H. Rzehak, G. Weiglein, Comput. Phys. Commun. **180**, 1426 (2009)
48. H. Bahl, T. Hahn, S. Heinemeyer, W. Hollik, S. Paßehr, H. Rzehak, G. Weiglein, Comput. Phys. Commun. **249**, 107099 (2020). arXiv:1811.09073 [hep-ph] see: www.feynhiggs.de
49. M. Awramik, M. Czakon, A. Freitas, G. Weiglein, Phys. Rev. D **69**, 053006 (2004). arXiv:hep-ph/0311148
50. G. Degrassi, P. Gambino, P.P. Giardino, *JHEP* **05**, 154 (2015). https://doi.org/10.1007/JHEP05(2015)154. arXiv:1411.7040 [hep-ph]
51. A. Freitas, S. Heinemeyer et al., arXiv:1906.05379 [hep-ph]
52. S. Heinemeyer, S. Jadach, J. Reuter, Eur. Phys. J. Plus **136**(9), 911 (2021). arXiv:2106.11802 [hep-ph]
53. S. Heinemeyer, W. Hollik, D. Stöckinger, A.M. Weber, G. Weiglein, JHEP **08**, 052 (2006). arXiv:hep-ph/0604147
54. S. Heinemeyer, W. Hollik, A.M. Weber, G. Weiglein, JHEP **04**, 039 (2008). arXiv:0710.2972 [hep-ph]
55. S. Heinemeyer, W. Hollik, G. Weiglein, L. Zeune, JHEP **12**, 084 (2013). arXiv:1311.1663 [hep-ph]
56. M. Endo, K. Hamaguchi, S. Iwamoto, T. Kitahara, JHEP **07**, 075 (2021). arXiv:2104.03217 [hep-ph]
57. S. Iwamoto, T.T. Yanagida, N. Yokozaki, Phys. Lett. B **823**, 136768 (2021). arXiv:2104.03223 [hep-ph]
58. Y. Gu, N. Liu, L. Su, D. Wang, Nucl. Phys. B **969**, 115481 (2021). arXiv:2104.03239 [hep-ph]
59. M. Van Beekveld, W. Beenakker, M. Schutten, J. De Wit, SciPost Phys. **11**(3), 049 (2021). arXiv:2104.03245 [hep-ph]
60. W. Yin, JHEP **06**, 029 (2021). arXiv:2104.03259 [hep-ph]
61. F. Wang, L. Wu, Y. Xiao, J.M. Yang, Y. Zhang, Nucl. Phys. B **970**, 115486 (2021). arXiv:2104.03262 [hep-ph]
62. M. Abdughani, Y.Z. Fan, L. Feng, Y.L. Sming Tsai, L. Wu, Q. Yuan, Sci. Bull. **66**, 2170–2174 (2021). arXiv:2104.03274 [hep-ph]
63. J. Cao, J. Lian, Y. Pan, D. Zhang, P. Zhu, JHEP **09**, 175 (2021). arXiv:2104.03284 [hep-ph]
64. M. Ibe, S. Kobayashi, Y. Nakayama, S. Shirai, arXiv:2104.03289 [hep-ph]
65. P. Cox, C. Han, T.T. Yanagida, Phys. Rev. D **104**(7), 075035 (2021). arXiv:2104.03290 [hep-ph]
66. C. Han, arXiv:2104.03292 [hep-ph]
67. S. Heinemeyer, E. Kpatcha, I. Lara, D.E. López-Fogliani, C. Muñoz, N. Nagata, Eur. Phys. J. C **81**(9), 802 (2021). arXiv:2104.03294 [hep-ph]
68. S. Baum, M. Carena, N.R. Shah, C.E.M. Wagner, arXiv:2104.03302 [hep-ph]
69. H.B. Zhang, C.X. Liu, J.L. Yang, T.F. Feng, arXiv:2104.03489 [hep-ph]
70. W. Ahmed, I. Khan, J. Li, T. Li, S. Raza, W. Zhang, arXiv:2104.03491 [hep-ph]
71. P. Athron, C. Balázs, D.H. Jacob, W. Kotlarski, D. Stöckinger, H. Stöckinger-Kim, JHEP **09**, 080 (2021). arXiv:2104.03691 [hep-ph]
72. A. Aboubrahim, M. Klasen, P. Nath, Phys. Rev. D **104**(3), 035039 (2021). arXiv:2104.03839 [hep-ph]
73. M. Chakraborti, L. Roszkowski, S. Trojanowski, JHEP **05**, 252 (2021). arXiv:2104.04458 [hep-ph]
74. H. Baer, V. Barger, H. Serce, Phys. Lett. B **820**, 136480 (2021). arXiv:2104.07597 [hep-ph]
75. W. Altmannshofer, S.A. Gadam, S. Gori, N. Hamer, arXiv:2104.08293 [hep-ph]
76. M. Chakraborti, S. Heinemeyer, I. Saha, arXiv:2105.06408 [hep-ph]
77. M.D. Zheng, H.H. Zhang, arXiv:2105.06954 [hep-ph]
78. K.S. Jeong, J. Kawamura, C.B. Park, JHEP **10**, 064 (2021). arXiv:2106.04238 [hep-ph]
79. Z. Li, G.L. Liu, F. Wang, J.M. Yang, Y. Zhang, arXiv:2106.04466 [hep-ph]
80. P.S.B. Dev, A. Soni, F. Xu, arXiv:2106.15647 [hep-ph]
81. J.S. Kim, D.E. Lopez-Fogliani, A.D. Perez, R.R. de Austri, arXiv:2107.02285 [hep-ph]
82. J. Ellis, J.L. Evans, N. Nagata, D.V. Nanopoulos, K.A. Olive, arXiv:2107.03025 [hep-ph]
83. S.M. Zhao, L.H. Su, X.X. Dong, T.T. Wang, T.F. Feng, arXiv:2107.03571 [hep-ph]
84. M. Frank, Y. Hiçyılmaz, S. Mondal, Ö. Özdal, C.S. Ün, JHEP **10**, 063 (2021). arXiv:2107.04116 [hep-ph]
85. Q. Shafi, C.S. Un, arXiv:2107.04563 [hep-ph]
86. S. Li, Y. Xiao, J.M. Yang, arXiv:2107.04962 [hep-ph]
87. A. Aranda, F.J. de Anda, A.P. Morais, R. Pasechnik, arXiv:2107.05495 [hep-ph]
88. A. Aboubrahim, M. Klasen, P. Nath, R.M. Syed, arXiv:2107.06021 [hep-ph]
89. Y. Nakai, M. Reece, M. Suzuki, JHEP **10**, 068 (2021). arXiv:2107.10268 [hep-ph]
90. T. Li, J.A. Maxin, D.V. Nanopoulos, arXiv:2107.12843 [hep-ph]
91. S. Li, Y. Xiao, J.M. Yang, Nucl. Phys. B **974**, 115629 (2022). arXiv:2108.00359 [hep-ph]
92. J.L. Lamborn, T. Li, J.A. Maxin, D.V. Nanopoulos, JHEP **11**, 081 (2021). arXiv:2108.08084 [hep-ph]
93. O. Fischer, B. Mellado, S. Antusch, E. Bagnaschi, S. Banerjee, G. Beck, B. Belfatto, M. Bellis, Z. Berezhiani, M. Blanke, et al., arXiv:2109.06065 [hep-ph]
94. A.K. Forster, S.F. King, arXiv:2109.10802 [hep-ph]
95. W. Ke, P. Slavich, arXiv:2109.15277 [hep-ph]
96. J. Ellis, J.L. Evans, N. Nagata, D.V. Nanopoulos, K.A. Olive, arXiv:2110.06833 [hep-ph]

97. P. Athron, C. Balázs, D. Jacob, W. Kotlarski, D. Stöckinger, H. Stöckinger-Kim, arXiv:2110.07156 [hep-ph]
98. M. Chakraborti, S. Heinemeyer, I. Saha, arXiv:2111.00322 [hep-ph]
99. S. Chapman, arXiv:2112.04469 [hep-ph]
100. A. Aboubrahim, M. Klasen, P. Nath, R.M. Syed, arXiv:2112.04986 [hep-ph]
101. I. Antoniadis, F. Rondeau, arXiv:2112.07587 [hep-th]
102. J.T. Acuña, P. Stengel, P. Ullio, arXiv:2112.08992 [hep-ph]
103. M.I. Ali, M. Chakraborti, U. Chattopadhyay, S. Mukherjee, arXiv:2112.09867 [hep-ph]
104. A. Djouadi, J.C. Criado, N. Koivunen, K. Müürsepp, M. Raidal, H. Veermäe, arXiv:2112.12502 [hep-ph]
105. K. Wang, J. Zhu, arXiv:2112.14576 [hep-ph]
106. F. Wang, W. Wang, J.M. Yang, Y. Zhang, B. Zhu, arXiv:2201.00156 [hep-ph]
107. M. Chakraborti, S. Heinemeyer, I. Saha, arXiv:2201.03390 [hep-ph]
108. M.A. Boussejra, F. Mahmoudi, G. Uhlrich, arXiv:2201.04659 [hep-ph]
109. R. Dermisek, arXiv:2201.06179 [hep-ph]
110. J. Cao, J. Lian, Y. Pan, Y. Yue, D. Zhang, arXiv:2201.11490 [hep-ph]
111. M.E. Gomez, Q. Shafi, A. Tiwari, C.S. Un, arXiv:2202.06419 [hep-ph]
112. W. Ahmed, I. Khan, T. Li, S. Raza, W. Zhang, arXiv:2202.11011 [hep-ph]
113. A. Chatterjee, A. Datta, S. Roy, arXiv:2202.12476 [hep-ph]
114. M. Chakraborti, S. Iwamoto, J.S. Kim, R. Masełek, K. Sakurai, arXiv:2202.12928 [hep-ph]
115. K. Agashe, M. Ekhterachian, Z. Liu, R. Sundrum, arXiv:2203.01796 [hep-ph]
116. P. Athron, C. Balazs, A. Fowlie, H. Lv, W. Su, L. Wu, J.M. Yang, Y. Zhang, arXiv:2203.04828 [hep-ph]
117. M. Endo, K. Hamaguchi, S. Iwamoto, S. i. Kawada, T. Kitahara, T. Moroi, T. Suehara, arXiv:2203.07056 [hep-ph]
118. S. Chigusa, T. Moroi, Y. Shoji, arXiv:2203.08062 [hep-ph]
119. H. Bahl, S. Heinemeyer, W. Hollik, G. Weiglein, Eur. Phys. J. C **80**(6), 497 (2020). arXiv:1912.04199 [hep-ph]
120. S. Heinemeyer, W. Hollik, G. Weiglein, Eur. Phys. J. C **9**, 343 (1999). arXiv:hep-ph/9812472
121. G. Degrassi, S. Heinemeyer, W. Hollik, P. Slavich, G. Weiglein, Eur. Phys. J. C **28**, 133 (2003). arXiv:hep-ph/0212020
122. T. Hahn, S. Heinemeyer, W. Hollik, H. Rzehak, G. Weiglein, Phys. Rev. Lett. **112**, 141801 (2014). arXiv:1312.4937 [hep-ph]
123. H. Bahl, W. Hollik, Eur. Phys. J. C **76**(9), 499 (2016). arXiv:1608.01880 [hep-ph]
124. H. Bahl, S. Heinemeyer, W. Hollik, G. Weiglein, Eur. Phys. J. C **78**(1), 57 (2018). arXiv:1706.00346 [hep-ph]
125. E. Bagnaschi et al., Eur. Phys. J. C **78**(3), 256 (2018). arXiv:1710.11091 [hep-ph]
126. P. Slavich, S. Heinemeyer (eds.), E. Bagnaschi et al., arXiv:2012.15629 [hep-ph]
127. W.G. Hollik, G. Weiglein, J. Wittbrodt, JHEP **03**, 109 (2019). arXiv:1812.04644 [hep-ph]
128. P.M. Ferreira, M. Mühlleitner, R. Santos, G. Weiglein, J. Wittbrodt, JHEP **09**, 006 (2019). arXiv:1905.10234 [hep-ph]
129. M. Drees, H. Dreiner, D. Schmeier, J. Tattersall, J.S. Kim, Comput. Phys. Commun. **187**, 227–265 (2015). arXiv:1312.2591 [hep-ph]
130. J.S. Kim, D. Schmeier, J. Tattersall, K. Rolbiecki, Comput. Phys. Commun. **196**, 535–562 (2015). arXiv:1503.01123 [hep-ph]
131. D. Dercks, N. Desai, J.S. Kim, K. Rolbiecki, J. Tattersall, T. Weber, Comput. Phys. Commun. **221**, 383–418 (2017). arXiv:1611.09856 [hep-ph]
132. M. Mühlleitner, A. Djouadi, Y. Mambrini, Comput. Phys. Commun. **168**, 46 (2005). arXiv:hep-ph/0311167
133. Joint LEP2 SUSY Working Group, the ALEPH, DELPHI, L3 and OPAL Collaborations. http://lepsusy.web.cern.ch/lepsusy/
134. G. Belanger, F. Boudjema, A. Pukhov, A. Semenov, Comput. Phys. Commun. **149**, 103–120 (2002). arXiv:hep-ph/0112278
135. G. Belanger, F. Boudjema, A. Pukhov, A. Semenov, Comput. Phys. Commun. **176**, 367–382 (2007). arXiv:hep-ph/0607059
136. G. Belanger, F. Boudjema, A. Pukhov, A. Semenov, Comput. Phys. Commun. **177**, 894–895 (2007). ([**134**])
137. G. Belanger, F. Boudjema, A. Pukhov, A. Semenov, arXiv:1305.0237 [hep-ph]
138. P. Athron et al., Eur. Phys. J. C **76**(2), 62 (2016). arXiv:1510.08071 [hep-ph]
139. P. von Weitershausen, M. Schafer, H. Stöckinger-Kim, D. Stöckinger, Phys. Rev. D **81**, 093004 (2010). arXiv:1003.5820 [hep-ph]
140. H. Fargnoli, C. Gnendiger, S. Paßehr, D. Stöckinger, H. Stöckinger-Kim, JHEP **1402**, 070 (2014). arXiv:1311.1775 [hep-ph]
141. M. Bach, J.H. Park, D. Stöckinger, H. Stöckinger-Kim, JHEP **1510**, 026 (2015). arXiv:1504.05500 [hep-ph]
142. S. Heinemeyer, D. Stöckinger, G. Weiglein, Nucl. Phys. B **690**, 62–80 (2004). arXiv:hep-ph/0312264
143. S. Heinemeyer, D. Stöckinger, G. Weiglein, Nucl. Phys. B **699**, 103–123 (2004). arXiv:hep-ph/0405255
144. P. Bechtle, S. Heinemeyer, O. Stål, T. Stefaniak, G. Weiglein, Eur. Phys. J. C **74**(2), 2711 (2014). arXiv:1305.1933 [hep-ph]
145. P. Bechtle, S. Heinemeyer, O. Stål, T. Stefaniak, G. Weiglein, JHEP **1411**, 039 (2014). arXiv:1403.1582 [hep-ph]
146. P. Bechtle, S. Heinemeyer, T. Klingl, T. Stefaniak, G. Weiglein, J. Wittbrodt, Eur. Phys. J. C **81**(2), 145 (2021). arXiv:2012.09197 [hep-ph]
147. P. Diessner, G. Weiglein, JHEP **07**, 011 (2019). arXiv:1904.03634 [hep-ph]
148. A. Sirlin, Phys. Rev. D **22**, 971–981 (1980)
149. W.J. Marciano, A. Sirlin, Phys. Rev. D**22** (1980), 2695 [Erratum: *Phys. Rev.***D 31** (1985), 213]
150. A. Djouadi, C. Verzegnassi, Phys. Lett. B **195**, 265–271 (1987)
151. A. Djouadi, Nuovo Cim. A **100**, 357 (1988)
152. B.A. Kniehl, Nucl. Phys. B **347**, 86–104 (1990)
153. F. Halzen, B.A. Kniehl, Nucl. Phys. B **353**, 567–590 (1991)
154. B.A. Kniehl, A. Sirlin, Nucl. Phys. B **371**, 141–148 (1992)
155. B.A. Kniehl, A. Sirlin, Phys. Rev. D **47**, 883–893 (1993)
156. F. Halzen, B.A. Kniehl, M.L. Stong, Z. Phys. C **58**, 119–132 (1993)
157. A. Freitas, W. Hollik, W. Walter, G. Weiglein, Phys. Lett. B**495**, 338–346 (2000). arXiv:hep-ph/0007091 [erratum: *Phys. Lett.***B 570** (2003) no.3-4, 265]
158. A. Freitas, W. Hollik, W. Walter, G. Weiglein, Nucl. Phys. B **632**, 189–218 (2002). arXiv:hep-ph/0202131 [Erratum: *Nucl. Phys.***B 666** (2003), 305–307]
159. M. Awramik, M. Czakon, Phys. Rev. Lett. **89**, 241801 (2002). arXiv:hep-ph/0208113
160. M. Awramik, M. Czakon, Phys. Lett. B **568**, 48–54 (2003). arXiv:hep-ph/0305248
161. A. Onishchenko, O. Veretin, Phys. Lett. B **551**, 111–114 (2003). arXiv:hep-ph/0209010
162. M. Awramik, M. Czakon, A. Onishchenko, O. Veretin, Phys. Rev. D **68**, 053004 (2003). arXiv:hep-ph/0209084
163. S. Bauberger, G. Weiglein, Nucl. Instrum. Methods A **389**, 318–322 (1997). arXiv:hep-ph/9611445
164. S. Bauberger, G. Weiglein, Phys. Lett. B **419**, 333–339 (1998). arXiv:hep-ph/9707510
165. M. Awramik, M. Czakon, A. Freitas, JHEP **11**, 048 (2006). arXiv:hep-ph/0608099

166. L. Avdeev, J. Fleischer, S. Mikhailov, O. Tarasov, Phys. Lett. B **336**, 560–566 (1994). arXiv:hep-ph/9406363 [hep-ph] [erratum: *Phys. Lett.***B 349** (1995), 597-598]
167. K.G. Chetyrkin, J.H. Kühn, M. Steinhauser, Phys. Lett. B **351**, 331–338 (1995). arXiv:hep-ph/9502291
168. K.G. Chetyrkin, J.H. Kühn, M. Steinhauser, Phys. Rev. Lett. **75**, 3394–3397 (1995). arXiv:hep-ph/9504413
169. K.G. Chetyrkin, J.H. Kühn, M. Steinhauser, Nucl. Phys. B **482**, 213–240 (1996). arXiv:hep-ph/9606230
170. M. Faisst, J.H. Kühn, T. Seidensticker, O. Veretin, Nucl. Phys. B **665**, 649–662 (2003). arXiv:hep-ph/0302275
171. J.J. van der Bij, K.G. Chetyrkin, M. Faisst, G. Jikia, T. Seidensticker, Phys. Lett. B **498**, 156–162 (2001). arXiv:hep-ph/0011373
172. R. Boughezal, J.B. Tausk, J.J. van der Bij, Nucl. Phys. B **713**, 278–290 (2005). arXiv:hep-ph/0410216
173. Y. Schroder, M. Steinhauser, Phys. Lett. B **622**, 124–130 (2005). arXiv:hep-ph/0504055
174. K.G. Chetyrkin, M. Faisst, J.H. Kühn, P. Maierhofer, C. Sturm, Phys. Rev. Lett. **97**, 102003 (2006). arXiv:hep-ph/0605201
175. R. Boughezal, M. Czakon, Nucl. Phys. B **755**, 221–238 (2006). arXiv:hep-ph/0606232
176. G. Weiglein, Acta Phys. Polon. B **29**, 2735–2741 (1998). arXiv:hep-ph/9807222
177. A. Stremplat, Diploma thesis (Univ. of Karlsruhe, 1998)
178. L. Chen, A. Freitas, JHEP **07**, 210 (2020). arXiv:2002.05845 [hep-ph]
179. L. Chen, A. Freitas, JHEP **03**, 215 (2021). arXiv:2012.08605 [hep-ph]
180. P.H. Chankowski, A. Dabelstein, W. Hollik, W.M. Mosle, S. Pokorski, J. Rosiek, Nucl. Phys. B **417**, 101–129 (1994)
181. A. Djouadi, P. Gambino, S. Heinemeyer, W. Hollik, C. Junger, G. Weiglein, Phys. Rev. Lett. **78**, 3626–3629 (1997). arXiv:hep-ph/9612363
182. A. Djouadi, P. Gambino, S. Heinemeyer, W. Hollik, C. Junger, G. Weiglein, Phys. Rev. D **57**, 4179–4196 (1998). arXiv:hep-ph/9710438
183. J. Haestier, S. Heinemeyer, D. Stöckinger, G. Weiglein, JHEP**12**, 027 (2005). arXiv:hep-ph/0508139
184. O. Stål, G. Weiglein, L. Zeune, JHEP **09**, 158 (2015). arXiv:1506.07465 [hep-ph]
185. M. Steinhauser, Phys. Lett. B **429**, 158–161 (1998). arXiv:hep-ph/9803313
186. K. Fujii et al. [LCC Physics Working Group], arXiv:1908.11299 [hep-ex]
187. M. Bicer et al., TLEP Design Study Working Group, JHEP **01**, 164 (2014). arXiv:1308.6176 [hep-ex]
188. A. Abada et al., FCC, Eur. Phys. J. ST **228**(2), 261–623 (2019)
189. J.B. Guimarães da Costa et al. [CEPC Study Group], arXiv:1811.10545 [hep-ex]
190. [CEPC Physics-Detector Study Group], arXiv:1901.03170 [hep-ex]
191. A. Djouadi, J.L. Kneur, G. Moultaka, Comput. Phys. Commun. **176**, 426 (2007). arXiv:hep-ph/0211331
192. G. Aad et al. [ATLAS], Eur. Phys. J. C **80**(2), 123 (2020). arXiv:1908.08215 [hep-ex]
193. M. Aaboud et al. [ATLAS], Eur. Phys. J. C **78**(12), 995 (2018). arXiv:1803.02762 [hep-ex]
194. T. Aaltonen et al., CDF, Science **376**(6589), 170–176 (2022)